Carboxyester hydrolysis promoted by dizinc(II) macrocyclic polyamine complexes with hydroxyethyl pendants: a model study for the role of the serine alkoxide nucleophile in zinc enzymes

Shu-An Li, De-Xi Yang, Dong-Feng Li, Jin Huang and Wen-Xia Tang*

State Key Laboratory of Coordination Chemistry, Nanjing University, Nanjing 210093,,
P.R. China. E-mail: wxtang@netra.nju.edu.cn

Received (in Montpellier, France) 31st May 2002, Accepted 16th July 2002
First published as an Advance Article on the web 5th November 2002

A novel dinuclear Zn(II) complex with hexaaza macrocycle bearing two hydroxyethyl pendants (L1), 3,6,9,16,19,22-hexaaza-6,19-bis(2-hydroxyethyl)-tricyclo[22,2,2,$2^{11,13}$]triaconta-1,11,13,24,27,29-hexaene), was synthesized as a model for alkaline phosphatase. The Zn(II) complex $[Zn_2L1(CH_3CO_2)_2](ClO_4)_2(H_2O)_2$ was isolated as a colorless crystal, triclinic, space group *P*-1. Both Zn(II) ions adopt the geometry of a distorted trigonal bipyramid in a pentacoordinated environment with Zn···Zn distance of 8.74 Å. The solution complexation study has revealed that the alcoholic hydroxyl group of the complex Zn_2L1 exhibits a low pK_a value at 25 °C. Zn(II)-bound alkoxides, which act as reactive nucleophiles toward the hydrolysis of 4-nitrophenyl acetate in 10% (v/v) CH_3CN at 25 °C, with $I = 0.10$ M ($NaNO_3$) and pH 9.0, have shown a second-order rate constant of 0.32 ± 0.01 $M^{-1}s^{-1}$, a value that is approximately 13 times greater than the value for the corresponding dinuclear Zn(II) complex formed by a hexaaza macrocycle without hydroxyethyl pendants (L2). The pH–rate profile for Zn_2L1 gave a sigmoidal curve. A possible mechanism has been proposed: the Zn(II)–RO^- function acts as a nucleophile in the first step of the hydrolytic mechanism, to give an acetyl intermediate, which is subsequently hydrolyzed to acetate by a Zn(II)–OH^- group.

Alkaline phosphatase catalytically hydrolyzes phosphate esters by using the two cooperative zinc(II) ions at the active center.[1] It is now accepted that one of the zinc ions may polarize a Ser-102 to yield a phosphoseryl-enzyme intermediate in the case of alkaline phosphatase, which subsequently is attacked by the adjacent Zn^{II}–OH^- to complete the hydrolysis and reproduce the free form of serine to reinitiate the catalytic cycle.[2] Recently, synthetic metal complexes acting as model compounds for hydrolytic metalloenzymes have attracted much attention.[3–7] Much of the effort to design synthetic nucleases or alkaline phosphatase to elucidate the mechanisms by which metal ions promote hydrolysis has focused primarily on mononuclear Zn(II) and Cu(II) complexes.[8–12] Kimura and co-workers studied the role of the alcohol pendant of the alcohol-pendant[$ZnH_{-1}L8$] and alcohol-pendant[12]aneN_4–Zn(II) complexes in the hydrolysis of carboxyl and phosphate esters.[8] Canary and other chemists have also been conducted modelling studies on the catalytic hydrolysis of carboxyl and phosphate esters.[9–12]

However, most of these models were mononuclear metal complexes, and only a few of the dinuclear complexes concentrate on the catalytic hydrolysis towards the substrate phosphodiester.[3–11] Furthermore, an enzyme always possesses the appropriate coordination geometry for metal ions with the appropriate rigidity and flexibility to accommodate the multiple requirements for the configuration of the active centers. In order to mimic the the active sites of these metallo-phosphodiesterases, chemists generally attempt to connect ligated metal ions by a molecular spacer in such way that the metal–metal distance matches with the anionic pentacoordinate phosphorus transition state. However, in contrast to nature enzymes, many of the low molecular weight model systems exhibit only minor catalytic activity due to lack of catalytic groups and too much rigidity or flexibility.[11b] Hence, we have utilized a macrocycle dinucleating ligand with two hydroxyethyl pendants containing *p*-xylyl spacers (see Chart 1, L1) as a molecular scaffold to construct a model complex for alkaline phosphatase, which made it possible to study the role of the Zn(II)–RO^- and Zn(II)–OH^- functions involved in the catalytic hydrolysis. In addition, incorporation of the *p*-xylyl spacers into a macrocycle reduces the flexibility of the macrocycle.[13] Indeed, we have found that the catalytic activity of Zn_2L1 is higher than that of Zn_2L2. Here we describe the synthesis and the crystal structure of the dinuclear Zn(II) complex of L1. The stability constants of Zn(II) complexes of L1 and catalytic carboxylester hydrolysis were also investigated.

Experimental

L1 was obtained by the condensation of 2-[bis(2-aminoethyl)amino]ethanol (L3) and terephthaldehyde and subsequent hydrogenation of the corresponding Schiff base according to the procedure reported previously by our group.[14] 3,6,9,16,19,22-hexaazatricyclo[22,2,2,$2^{11,13}$]triaconta-1,11,13,24,27,29-hexaene(L2) and L3 were synthesized as described previously in the literature.[15,16] The other reagents were of analytical grade from commercial sources and were used without any further purification. C, H and N analyses were made on a Perkin–Elmer 240C elemental analyzer. Electrospray mass (ES-MS) spectral measurements were carried out on a LCQ System (Finngan MAT, USA) using methanol as the mobile phase. The spray voltage and capillary temperature were set at 4.5 kV and 200 °C, respectively.

Preparations

$[Zn_2L1(CH_3CO_2)_2](ClO_4)_2(H_2O)_2$, I. A 0.108 g (0.217 mmol) amount of L1 was dissolved in 4 mL of water, to which

DOI: 10.1039/b205302k

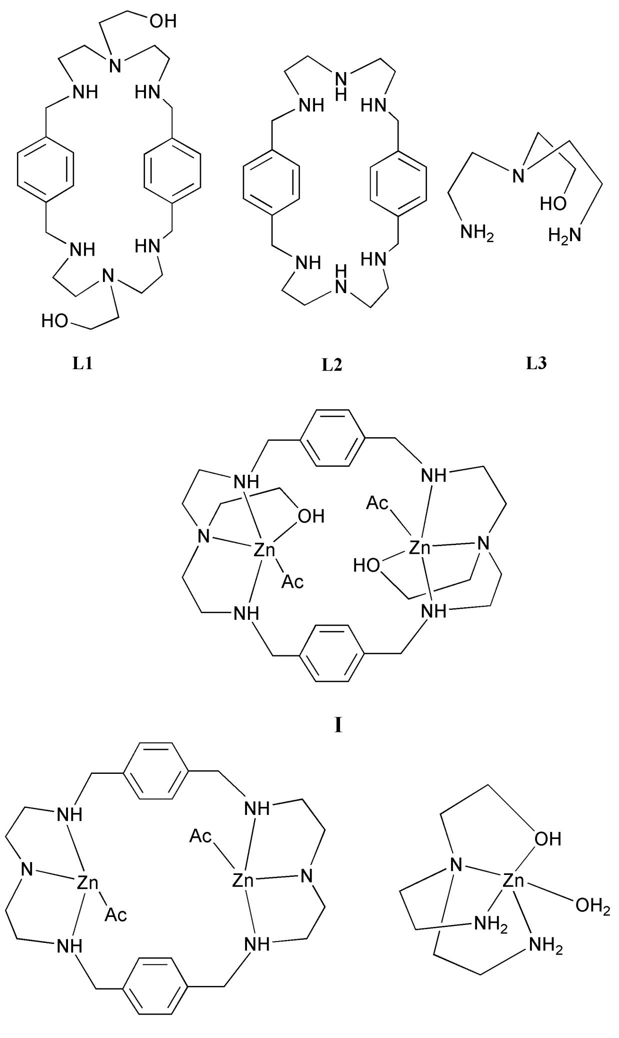

Chart 1

0.1904 g (0.434 mmol) $Zn(CH_3CO_2)_2{\cdot}2H_2O$ and 3 mL water was added with stirring. Then, 1 mL saturated $NaClO_4$ solution was added to the solution, from which a white residue was obtained. The residue was dissolved in 5 mL CH_3CN and stirred overnight, the solution was filtered and the filtrate was placed in the air to evaporate at ambient temperature. A few days later, several colorless block crystals were obtained in 53% yield. Anal. calcd for $C_{32}H_{56}N_6O_{16}Cl_2Zn_2$: C, 39.12; H, 5.74; N, 8.55%. Found : C, 39.19; H, 5.63; N, 8.47%.

$[Zn_2L1Cl_2]Cl_2 \cdot 2H_2O$. In order to avoid the interference of the coordinated acetate, we use $[Zn_2L1Cl_2]^{2+}$ instead of $[Zn_2L1(CH_3CO_2)_2]^{2+}$ in the course of capture of the acetyl intermediate. The preparation of $[Zn_2L1Cl_2]^{2+}$ was as follows: to an aqueous solution (2 mL) containing $ZnCl_2{\cdot}2H_2O$ (0.0341 g, 0.20 mmol), a solution of L1(0.0498 g, 0.10 mmol) in H_2O (2 mL) was added dropwise with stirring at 60 °C; after being stirred for 2 h, the reaction mixture was filtrated. A colorless block crystal was obtained by slow evaporation of the filtrated solution for several days at ambient temperature. Anal. calcd for $Zn_2L1Cl_4{\cdot}2H_2O$ (807.3): C, 41.66; H, 6.24; N, 10.41%. Found: C, 41.69; H, 6.33; N, 10.67%. ES-MS: $m/z = 735.1$ for $[Zn_2L1Cl_3]^+$.

$Zn_2L2(CH_3CO_2)_2](CH_3CO_2)_2 \cdot 2H_2O$ II. The dizinc complex of L2 was also prepared for determination of its rate of catalytic hydrolysis as a comparison with Zn_2L1. A solution of 0.1221 g (0.298 mmol) L2 and 5 mL methanol was added dropwise to a methanol solution (10 mL) of $Zn(CH_3CO_2)_2{\cdot}2H_2O$ (0.1308 g, 0.596 mmol) with stirring. Then, 2 drops of triethylamine were added to the solution to adjust the pH to *ca.* 8.5 and the resulting solution was filtered. The filtrate was allowed to react for 2 h. Afterward, the white precipitate was obtained (yield: 46%) by evaporation of the filtrated solution at ambient temperature for a week. Anal. calcd. for $C_{32}H_{54}N_6O_{10}Zn_2$ (813.58): C, 47.24; H, 6.69; N, 10.33%. Found: C, 47.61; H, 6.60; N, 10.48%. Es-MS: $m/z = 797.0$ for $[Zn_2L2(CH_3CO_2)_3(CH_3OH)_2(H_2O)]^+$.

Caution! *Perchlorate salts of compounds containing organic ligands are potentially explosive, especially when heated or bumped. Only small quantities of these compounds should be prepared and handled behind suitable protective shields.*

X-Ray crystal structure determination

The colorless crystals were mounted on a glass fiber. The data collections were performed on a CAD4 X-ray diffractometer with graphite-monochromated Mo $K\alpha$ radiation ($\lambda = 0.71073$ Å) using $\omega/2\theta$ scan mode at 293 K in the range $2.15° \leqslant \theta \leqslant 24.97°$. The structure was solved by direct methods using SHELXS-97 and refined by full-matrix least-squares calculation on F^2 with SHELXL-97.[17,18] All non-hydrogen atoms were refined anisotropically. Full-matrix least-squares methods were used to refine an overall scale factor, positional and thermal parameters.

CCDC reference number 194457. See http://www.rsc.org/suppdata/nj/b2/b205302k/ for crystallographic files in CIF or other electronic format.

Potentiometry

Potentiometric studies were conducted with an Orion 91-04 glass combination pH electrode and an Orion microprocessor ionalyzer/901 at 25 °C. All solutions were carefully protected from air by a stream of humidified nitrogen gas. Standard NaOH (CO_2-free) was added by a spiral micro-injector. The $ZnCl_2$ solution was calibrated by standard EDTA. Doubly distilled water with a pH value of about 6 was used. The temperature of the cell was controlled by a thermostat. K_w was taken to be 13.69 at 25 °C. NaCl (0.1 M) was added to adjust the ionic strength to 0.10 M. Solutions containing 1 mmol L1 with or without 2 mmol $ZnCl_2{\cdot}2H_2O$ were titrated to pH > 11. The complexation and protonation constants were calculated using the program BEST.[19] All data represent the average of at least two independent experiments and all the sigma fit values have been reduced to less than 0.023 after optimization.

Kinetic studies

The catalytic hydrolysis rate of 4-nitrophenyl acetate (NA) by the $[Zn_2L1(CH_3CO_2)_2]^{2+}$ complex was measured by the initial slope method, following the increase in the 400 nm absorption of released 4-nitrophenolate (NP) in 10% CH_3CN (v/v) aqueous solution at 25 °C. Buffer solutions containing 20 mM tris buffer (pH 7.5–8.7) and CHES (pH 9.0–9.3) were used, and the ionic strength was adjusted to 0.10 M with 1 M $NaNO_3$. The initial rate determination was carried out according to the typical procedure previously reported by Kimura and our group.[8] NA and a Zn(II) complex were mixed in the buffered solution, the UV absorption increase recorded immediately on the UV-3100 and then followed generally until *ca.* 0.1% formation of 4-nitrophenolate. The observed first-order rate constant $k_{obsd}(s^{-1})$ was calculated from the decay slope (NP release rate/[NP]). The value of $k_{obsd}/[Zn^{II}\ complex]_{total}$ gave the second-order rate constant $k_{NA}(M^{-1}\ s^{-1})$ for NA hydrolysis.

To check if the NA hydrolysis was catalytic, substrate saturation kinetics were performed at pH = 8.5 (buffered with

Table 1 Crystallographic data for dizinc complexes **I**

Formula	$C_{32}H_{56}Cl_2N_6O_{16}Zn_2$
FW	982.47
Crystal system	Triclinic
Space group	$P\bar{1}$
T/K	293(2)
λ/Å	0.71073
a/Å	8.7320(17)
b/Å	9.807(2)
c/Å	12.723(3)
α/deg	75.09(3)
β/deg	78.35(3)
γ/deg	86.02(3)
U/Å^3	1031.0(4)
Z	1
μ/mm^{-1}	1.369
Reflns collcd	3873
Indep. reflns	3613
R(int)	0.0259
$R_1{}^a$ $[I > 2\sigma(I)]$	0.0334
$wR_2{}^b$ $[I > 2\sigma(I)]$	0.0749

[a] $R_1 = \sum\|F_o| - |F_c\|/\sum|F_o|$, $wR_2 = |\sum w(|F_o|^2 - |F_c|^2)|/\sum|w(F_o)^2|^{1/2}$,
[b] $w = 1/[(F_o{}^2)^2 + (0.0377P)^2 + 1.5300P]$, where $P = (F_o{}^2 + 2F_c{}^2)/3$,

tris) and 25 °C with an ionic strength of 0.1 M (adjusted with $NaNO_3$).[8c] The NA concentration utilized was 6.0 mM, while the metal complex concentration was 0.2 mM for $[Zn_2L1(CH_3CO_2)_2]^{2+}$. All the experiments were run twice, and the tabulated data represent the average of these experiments. For a comparison, the rates of hydrolysis for $[Zn_2H_2L2]^{2+}$ were also measured at pH = 9.3 using the same procedure described above.

Results and discussion

X-Ray structure of $[Zn_2L1(CH_3CO_2)_2](ClO_4)_2(H_2O)_2$, I

The crystal structure of the dizinc complex **I** consists of the cationic unit $[Zn_2L1(CH_3CO_2)]^{2+}$, perchlorate anions and crystallization water molecules. The crystal data and structural refinement parameters are displayed in Table 1. Selected bond lengths and angles are presented in Table 2. Fig. 1 shows an ORTEP drawing of the structure of dizinc complex **I** with 30% probability thermal ellipsoids. The crystal structure belongs to the space group $P\bar{1}$ with the crystallographic inversion center located in the macrocyclic cavity. Each macrocycle binds two Zn(II) ions by its diethylenetriamine moieties, which provide three nitrogen donors to each Zn(II) ion, and the rest of the coordinated atoms are oxygen atoms, one is from acetate anion and the another is from the hydroxyethyl pendant. The Zn1 atom lies 0.386 Å below the trigonal equatorial plane formed by O1, N2 and N3 with O1–Zn1–N2 = 117.7°, N3–Zn1–O1 = 118.1°, and N2–Zn1–N3 = 115.1°, while the two axial sites are occupied by N1 and O2 with O2–Zn1–N1 = 162.8°. The distortion (Δ) of the coordination polyhedron from a regular trigonal-bipyramid (TBP, $\Delta = 0$) to the tetragonal pyramid ($\Delta = 1$) has been calculated according to the literature reported by Mutterties and Galy and their coworkers.[20,21] The value of 0.23 found indicates that the coordination geometry around Zn(II) is much closer to TBP. The two Zn(II) ions lie 8.74 Å apart. Two phenyl rings in the Zn(II) complex (**I**) are parallel to each other with a center distance of 5.32 Å.

Table 2 Selected bond distances (Å) and angles (°) for **I**

Zn1–O1	2.066(3)	Zn1–O2	2.012(2)
Zn1–N1	2.237(3)	Zn1–N2	2.084(3)
Zn1–N3	2.110(3)		
O2–Zn1–O1	87.58(11)	O2–Zn1–N2	111.91(10)
O1–Zn1–N2	117.65(12)	O2–Zn1–N3	100.91(10)
O1–Zn1–N3	118.13(13)	N2–Zn1–N3	115.09(12)
O2–Zn1–N1	162.77(10)	O1–Zn1–N1	76.48(11)
N2–Zn1–N1	81.80(11)	N1–Zn1–N3	81.37(11)

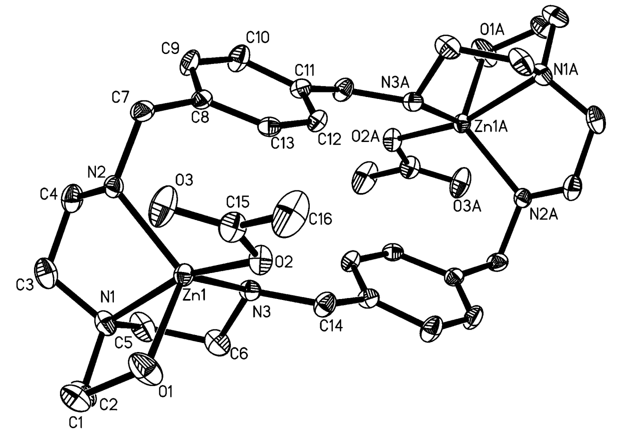

Fig. 1 An ORTEP drawing (30% probability ellipsoids) of $[Zn_2L1(CH_3CO_2)_2]^{2+}$. All hydrogen atoms, perchlorate anions and crystalline water molecules are omitted for clarity.

Zn(II) complexation constants of L1

The Zn(II) complexation constants of the macrocyclic ligand L1 were determined by potentiometric titration. Protonation constants of the ligand L1 have been reported in our previous paper.[14] When 2 mole equiv. of Zn(II) were added to the solution, the titration curve reveals two inflexions at $a = 2$ and $a = 8$, respectively, as shown in Fig. 2(b). The inflexion at $a = 2$, as in Fig. 2(a) or 2(b), indicates that the two tertiary nitrogen atoms are of very low basicity and release their protons easily into aqueous solution at low pH. The inflection $a = 8$ corresponds to the completion of the neutralization of the six ammonium ions in the diethylenetriamine moieties and the deprotonation of another two titratable protons from two hydroxyethyl pendants bound to Zn(II). Table 3 summarizes the obtained formation constants of the Zn(II) complexes with L1, in comparison with the previously reported constants of L3.

The most significant finding is the extremely facile deprotonation of the alcoholic function with pK_{a1} = 7.72 at 25 °C, which is similar to the value for the mononuclear ZnL2 complex (pK_{a1} = 7.74, Table 3) and close to that found by Kimura *et al.* for the Zn(II) complex (pK_{a1} = 7.40 at 25 °C), and which

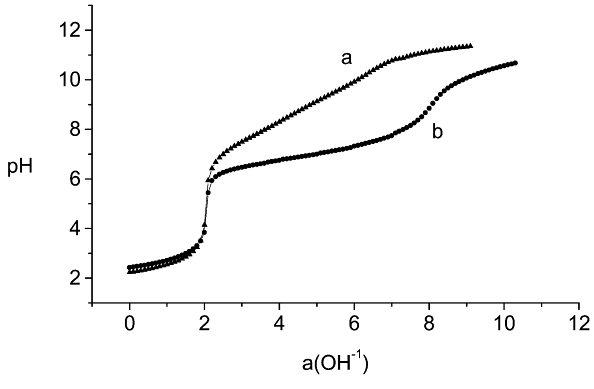

Fig. 2 (a) The potentiometric titration curves for L1·6HBr. (b) For 2:1 molar ratios of Zn(II):L1·6HBr (a = mole of NaOH added per mole of ligand, I = 0.10 M at = 25 °C), the fit value is 0.023.

Table 3 Comparison of Zn(II) complexation constants of the two ligands L1 and L3 and deprotonation constants of the corresponding complexes with $I = 0.1$ at $25 \pm 0.1\,°C$

Reaction	log K	
	L1	L3
$L1 + Zn^{2+} \leftrightharpoons ZnL1^{2+}$	17.12	9.41[a]
$ZnL1^{2+} + H^+ \leftrightharpoons ZnHL1^{3+}$	7.14	–
$ZnHL1^{3+} + H^+ \leftrightharpoons ZnH_2L1^{4+}$	6.94	–
$ZnL1^{2+} + Zn^{2+} \leftrightharpoons Zn_2L1^{4+}$	11.80	–
pK_{a1}	7.72[b]	7.74[a]
pK_{a2}	7.81[b]	9.78[a]
pK_{a3}	9.49[b]	
pK_{a4}	10.16[b]	

[a] From ref. 12*a*, for L3, K_{a1} is relative to the equilibria $ZnL3^{2+} \leftrightharpoons ZnH_{-1}L3^+ + H^+$. K_{a2} is relative to the equilibria $ZnH_{-1}L3^+ \leftrightharpoons ZnH_{-1}L3(OH)^+ + H^+$. [b] For L1, K_{a1} is relative to the equilibria $Zn_2L1^{4+} \leftrightharpoons Zn_2H_{-1}L1^{3+} + H^+$. K_{a2} is relative to the equilibria $Zn_2H_{-1}L1^{3+} \leftrightharpoons Zn_2H_{-2}L1^{2+} + H^+$. K_{a3} is relative to the equilibria $Zn_2H_{-2}L^{2+} \leftrightharpoons Zn_2H_{-2}L1(OH)^+ + H^+$. K_{a4} is relative to the equilibria $Zn_2H_{-2}L1(OH)^+ \leftrightharpoons Zn_2H_{-2}L1(OH)_2 + H^+$.

implies that the title complex is a stronger nucleophile to attack an ester bond in catalytic hydrolysis.[8c] In addition, the value of log$K$(ZnL1) (17.12) for L1 and the Zn(II) system is higher than the corresponding value for L3 and the Zn(II) system (9.41),[12a] indicating that the macrocyclic ligand (L1) binds more strongly to metal ions than L3.

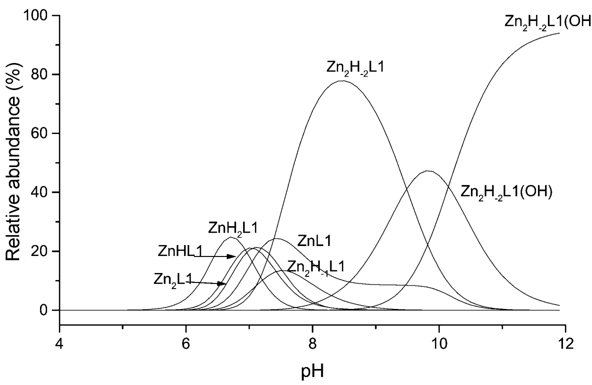

Fig. 3 Species distribution graph as a function of pH for the 1.0 mM L1·6HBr + 2.0 mM Zn(II) system at 25 °C and $I = 0.1$ M ($NaClO_4$).

Fig. 3 displays the species distribution as a function of pH for [total Zn(II)] = 2 mM, [total L1] = 1 mM at 25 °C. The dinuclear complex $[Zn_2L1]^{4+}$ is formed over the pH range 6–8.5 (maximum at pH 7.1, 20.1%). The $[Zn_2H_{-1}L1)]^{3+}$ ion is formed over pH 6.5–9.4 and $[Zn_2H_{-2}L1]^{2+}$ predominates over pH 7.3–9.3. The $[Zn_2H_{-2}L1]^{2+}$ species is further deprotonated stepwise to yield $[Zn_2H_{-2}L1(OH)]^+$ and $[Zn_2H_{-2}L1(OH)_2]$, respectively. The structural formulae of the major species are displayed in Scheme 1.

4-Nitrophenyl acetate (NA) hydrolysis promoted by Zn_2L1

As a model for the active center in Zn(II)-containing hydrolytic enzymes, especially alkaline phosphatase, the catalytic activity of the Zn_2L1 complex has been tested. Since the phosphomonoesters underwent only slow hydrolysis with Zn_2L1, similar

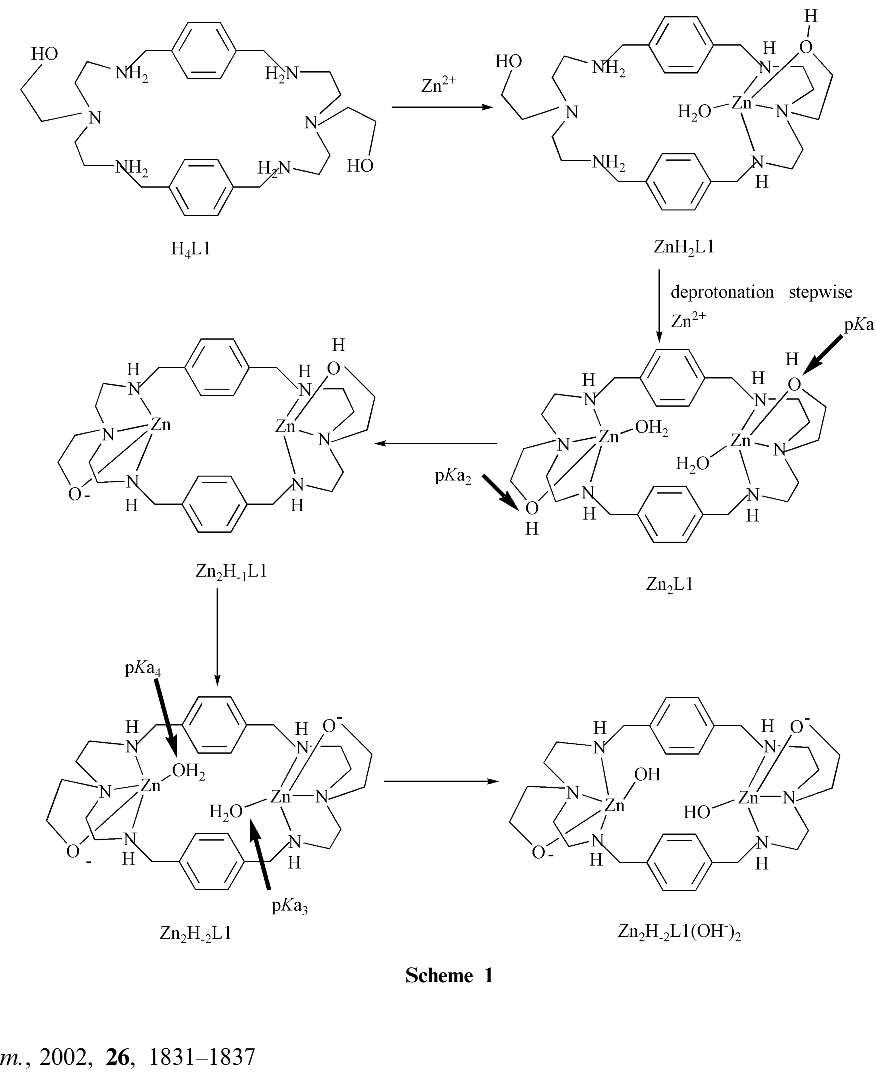

Scheme 1

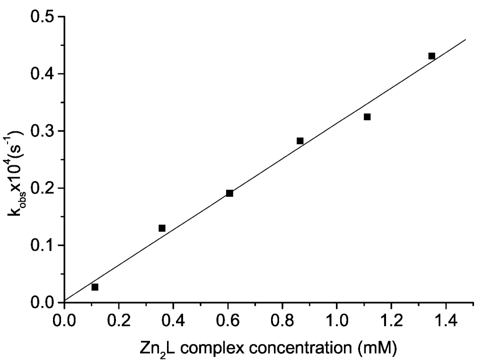

Fig. 4 Typical dependence of observed pseudo-first-order rate constants for hydrolysis of NA on the total concentration of Zn_2L1 with $I = 0.1$ M ($NaNO_3$) at 25 °C in the presence of 10% (v/v) CH_3CN; correlation coefficient > 0.99.

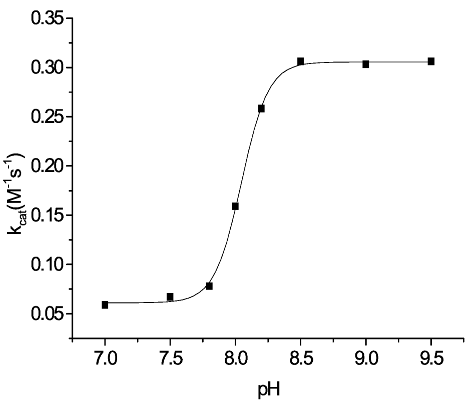

Fig. 5 pH–rate profile for the second-order rate constants of NA hydrolysis with Zn_2L1 complex at 25 °C and $I = 0.1$ M ($NaNO_3$) in 10% (v/v) CH_3CN.

to that with other Zn(II) or Cu(II) complexes, the carboxylester 4-nitrophenyl acetate (NA) was used as a substitute.[8c,22,23] The second-order kinetics of Zn_2L1 promoted NA hydrolysis was followed at different pH values. The initial rate constant k_{in}, observed rate constant k_{obs}, the spontaneous hydrolysis constant v_{buffer} and the second-order constant k_{cat} are defined as follows:

$$v_{total} = v_{Zn2L} + v_{buffer} = k_{in}[NA]$$

$$v_{Zn2L} = k_{obs}[Zn(II)\ COMPLEX]_{total} \cdot [NA]$$

$$v_{buffer} = (k_{OH^-}[OH^-] + \cdots) \cdot [NA]$$

The second-order rate constant k_{cat} for Zn_2L1 is 0.32 M^{-1} s^{-1} at pH = 9.0, calculated from the slope of the straight line k_{obs} *vs.* $[Zn(II)\ complex]_{total}$ (see Fig. 4), and the relative k_{cat} values of NA hydrolysis catalyzed by some other Zn(II) complexes are listed in Table 4.

To examine whether the whole process is catalytic hydrolysis or transesterification, we followed the release of NP up to more than one circle with the NA concentration fixed at 6.0 mM and the Zn(II) complex concentration only 0.2 mM in buffer solution (pH = 9.3), following the absorbance at 400 nm at 25 °C. The resulting v_{total} *vs.* time curve revealed that the rate constant for Zn_2L1 was identical to the initial rate constant determined above. Thus, the mechanism is catalytic hydrolysis instead of transesterification. As indicated in Table 4, the Zn_2L1^{4+} complex is one of the most active catalysts for NA hydrolysis. The first-order constants (k_{cat}) are plotted as a function of pH, and the resulting sigmoidal curve is shown as Fig. 5. This curve is characteristic of a kinetic process controlled by an acid-base equilibrium with an inflexion point at pH = 8.0, which is close to the pK_{a2}(7.81) and pK_{a1}(7.72) values for the deprotonation of the hydroxyethyl pendants of the Zn_2L1 complex that were measured by potentiometric pH titration in 10% (v/v) CH_3CN. Therefore, the main promoter species are concluded to be the deprotonated species $[Zn_2H_{-2}L1]^{2+}$ and $[Zn_2H_{-2}L1(OH)]^{2+}$.

Table 4 Comparison of hydrolysis rate constants, k_{cat} (M^{-1} s^{-1}), for Zn_2L1 and other complexes at $I = 0.1$ M ($NaNO_3$), pH = 9.0 and 25 °C in 10%(v/v) CH_3CN

Promoter[a]	k_{cat}
$[Zn_2L1]^{4+}$	0.32 ± 0.02
$[Zn_2L2]^{4+}$	0.024 ± 0.01
$[ZnH_{-1}L3]^+$	0.13 ± 0.01[b]
$[Zn_2H_{-1}L6]^{3+}$	0.21[c]
$[Zn_2L7(OH)]^{3+}$	0.094[c]
$[ZnH_{-1}L8]^+$	0.14[d]

[a] The actual nucleophiles are deprotonated Zn(II)complexes. [b] From ref. 12*a*. [c] From ref. 11*a*, where L6 is 4-(2-hydroxyethyl)-1,4,7,16,19,22-hexaaza-10,13,25,28-tetraoxacyclotriacontane, L7 is 1,4,7,16,19,22-hexaaza-10,13,25,28-tetraoxacyclotriacontane. [d] From ref. 8*c*, L8 is 1-hydroxyethyl-1,5,9-triazacyclodododecane.

To further investigate the role of the hydroxyethyl pendants in the title compound in the catalytic ester hydrolysis, the rate constant of NA hydrolysis catalyzed by a Zn(II) complex containing the corresponding macrocyclic ligand without hydroxyethyl pendants (Zn_2L2) was also determined, giving $k_{cat} = 0.024$ M^{-1} s^{-1} at pH 9.0 (see Table 4), in which Zn(II)–OH^- is only an active nucleophile. Comparing the kinetic data for both Zn_2L1 and Zn_2L2, the rate constant of Zn_2L1 is approximately 13 times greater than the corresponding value of Zn_2L2. These results suggest that a Zn(II)-bound alkoxide is a better nucleophile than a Zn(II)-bound hydroxide.

It is worth pointing out that the rate constant of Zn_2L1 is approximately 2.4 times greater than the corresponding value ($k_{cat} = 0.13$ M^{-1} s^{-1}) of the ZnL3 complex(see Table 4), that is, the actives are nearly two times higher than their mononuclear analogs, which demonstrates that there is no remarkable cooperation in carboxyester hydrolysis between two Zn(II) ions in the active centers of the model complex Zn_2L1, due to the long Zn···Zn distance revealed by the X-ray analysis above.

In the course of catalytic NA hydrolysis, we suspected that a transient "acetyl intermediate" was formed, which then disappeared very rapidly to give the final product acetate anion and Zn_2L1. Because the lifetimes of the acetyl intermediates **IV** and **V** (see Scheme 2) were too short to permit their isolation from an aqueous buffer solution (pH 9.0), a nonbuffer solution was used to prevent the following intramolecular acetate hydrolysis. Following a similar procedure as that described by Kimura *et al.*,[8c] the acetyl intermediate **IV** or **V** was independently confirmed by isolation of the Zn^{II}-free ligands L4 and L5 from the reaction of NA with $[Zn_2L1Cl_2]Cl_2 \cdot 2H_2O$ in CH_3CN, followed by addition of aqueous EDTA solution to the reaction mixture and then extraction with CH_2Cl_2 to give a mixture of L1 and L4 and L5. The isolation details of L4 and L5 are as follows: $[Zn_2L1Cl_2]Cl_2 \cdot 2H_2O$ (0.1615 g, 0.2 mmol) and 4-nitrophenyl acetate (0.0906 g, 0.50 mmol) were dissolved in 10 mL CH_3CN and stirred at room temperature for 10 h. After evaporation of the solvent, an aqueous solution (20 mL) of EDTA (0.66 g, 1.78 mmol) was added to the residue. The solution pH was adjusted to 9 with 1 M NaOH aqueous solution, and then the solution was extracted with CH_2Cl_2 (25 mL × 2). After the organic solvent was evaporated, a white powder was obtained and analyzed by ES-MS. As shown in Fig. 6, the peaks at $m/z = 499.4$ (32%), 541.5 (11%) and 583.4 (100%) are assigned to $[L1H]^+$, $[L4H]^+$ and $[L5H]^+$, respectively. On this basis, we propose the possible overall catalytic reaction depicted in Scheme 2, in which the slowest step is the initial

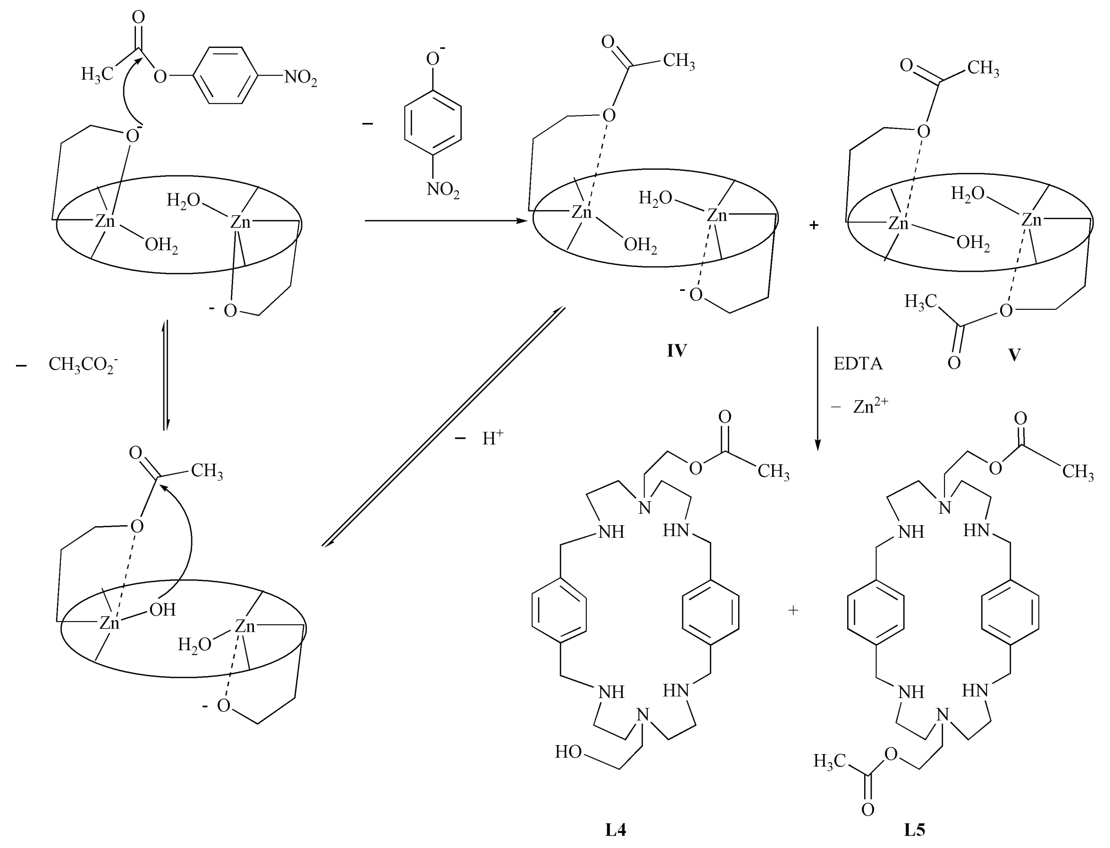

Scheme 2

formation of the acetyl intermediate. The formation of a similar intermediate was also observed by the groups of Kimura, Bencini and ours in NA hydrolysis catalyzed by mononuclear and dinuclear Zn(II) complexes.[8c,11a,12a] The acetyl intermediate is subsequently hydrolyzed through the intramolecular nucleophilic attack of a coordinated water molecule at neutral pH or by a more strongly nucleophile Zn(II)–OH function generated at alkaline pH. It is to be noted, as in alkaline phosphatase, that both the nucleophilic RO$^-$–Zn(II) and Zn(II)–OH$^-$ functions are involved in this hydrolytic process.

Conclusion

A novel dinuclear Zn(II) complex of a macrocyclic ligand with two hydroxyethyl pendants has been synthesized. The solution complexation study by potentiometric titration on the Zn(II) complexes of L1 has revealed that the Zn$_2$L1 complex is formed, which has low pK_a values of 7.7 and 7.8 at 25 °C and $I = 0.1$ M (NaNO$_3$). X-Ray diffraction analysis of the title complex indicates that both Zn(II) ions adopt a trigonal-bipyramid geometry with a Zn···Zn distance of 8.74 Å. The 4-nitrophenyl acetate hydrolysis promoted by the Zn$_2$L1 complex showed a second-order rate constant of 0.32 M^{-1} s^{-1}, which is approximately 13 times greater than that of Zn$_2$L2. The preference of the Zn(II)–alkoxide catalyzed ester hydrolysis over Zn(II)–hydroxide catalytic hydrolysis was proved by kinetic experiments and provides evidence for the stronger nucleophilic ability of Zn(II)–alkoxide than Zn(II)–hydroxide. In the catalytic reaction, the RO$^-$–Zn(II) function acts as a nucleophile in the first step of NA hydrolysis, giving an acetyl intermediate, which is subsequently hydrolyzed *via* an intramolecular attack of a Zn(II)–OH function. However, intermolecular attack by external water or hydroxide should not be ruled out.

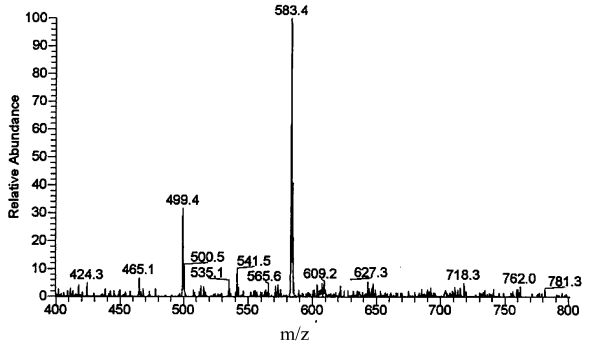

Fig. 6 Electrospray mass spectrum of the mixture of L1 and Zn^{II}-free ligands L4 and L5.

Acknowledgements

This work is supported by the National Natural Science Foundation of China.

References

1 N. Sträter, W. N. Lipscomb, T. Klablunde and B. Kreb, *Angew. Chem., Int. Ed. Engl.*, 1996, **35**, 2024–2055.
2 (*a*) D. E. Fenton and H. J. Okawa, *J. Chem. Soc., Dalton Trans.*, 1993, 1349–1357; (*b*) B. L. Vallee and D. S. Auld, *Acc. Chem. Res.*, 1993, **26**, 543–551.
3 D. M. Perreault and E. V. Anslyn, *Angew. Chem., Int. Ed. Engl.*, 1997, **36**, 433–450.
4 N. H. Williams, B. Takasaki, M. Wall and J. Chin, *Acc. Chem. Res.*, 1999, **32**, 485–493.
5 M. W. Göbel, *Angew. Chem., Int. Ed. Engl.*, 1994, **33**, 1141–1143.
6 J. Chin, *Acc. Chem. Res.*, 1991, **24**, 145–149.
7 D. E. Wilcox, *Chem. Rev.*, 1996, **96**, 2435–2441.
8 (*a*) E. Kimura and E. Kikuta, *J. Biol. Inorg. Chem.*, 2000, **5**, 139–155; (*b*) T. Koile, S. Kajitan, I. Nakamura, E. Kimura and M. Shiro, *J. Am. Chem. Soc.*, 1995, **117**, 1210–1219; (*c*) E. Kimura, I. Nakamura, T. Koike, M. Shionaoya, Y. Kodama, T. Ikeda

and T. Shiro, *J. Am. Chem. Soc.*, 1994, **116**, 4764–4771.(*d*) E. Kimura, M. Shionoya, A. Hoshino, T. Ikeda and Y. Yamada, *J. Am. Chem. Soc.*, 1992, **114**, 10 134–10 137.

9 (*a*) J. W. Canary, J. Xu, J. M. Castagnetto, D. Rentzeperis and L. A. Marky, *J. Am. Chem. Soc.*, 1995, **117**, 11 545–11 547; (*b*) X. Xu, A. R. Lajmi and J. W. Canary, *Chem. Commun.*, 1998, 2701–2702.

10 (*a*) M. J. Young, D. Wajnon, R. C. Hynes and J. Chin, *J. Am. Chem. Soc.*, 1995, **117**, 9441–9447; (*b*) J. Chin and M. Banaszczyk, *J. Am. Chem. Soc.*, 1989, **111**, 2724–2726; (*c*) J. A. Connolly, M. Banaszczyk, R. C. Hynes and J. Chin, *Inorg. Chem.*, 1994, **33**, 665–669; (*d*) J. Chin and V. Jubian, *J. Chem. Soc., Chem. Commun.*, 1989, 839–841; (*e*) J. H. Kim and J. Chin, *J. Am. Chem. Soc.*, 1992, **114**, 9792–9795; (*f*) E. L. Hegg, E. V. Mortimore, C. L. Cheung, J. E. Huyett, D. R. Powell and J. N. Burstyn, *Inorg. Chem.*, 1999, **38**, 2961–2968.

11 (*a*) C. Bazzicalpi, A. Bencini, E. Berni, A. Bianchi, V. Fedi, V. Fusi, C. Giorgi, P. Paoletti and B. Valtancoli, *Inorg. Chem.*, 1999, **38**, 4115–4122; (*b*) P. Molenveld, J. F. J. Engbersen and D. N. Reinhouldt, *Chem. Soc. Rev.*, 2000, **29**, 75–86.

12 (*a*) J. Xia, Y. Xu, S. Li, K. Yu and W. Tang, *Inorg. Chem.*, 2001, **40**, 2394–2401; (*b*) J. Xia, S. Li, Y. Shi, K. Yu and W. Tang, *J. Chem. Soc., Dalton Trans.*, 2001, 2109–2115.

13 C. Bazzicalupi, A. Bencini, A. Bianchi, V. Fusi, C. Giorgi, P. Paoletti, A. Stefani and B. Valtancoli, *Inorg. Chem.*, 1995, **34**, 552–559.

14 S. Li, J. Xia, D. Yang, Y. Xu, D. Li, M. Wu and W. Tang, *Inorg. Chem.*, 2002, **41**, 1807–1815.

15 V. A. Bobylev and V. O. Chechik, *Zh. Obshch. Khim.*, 1990, **60**, 2721–2725.

16 D. Chen and A. E. Martell, *Tetrahedron*, 1991, **47**, 6895–6902.

17 Siemens, XSCANS (v. 2.1), Siemens Analytical X-Ray Instruments, Madison, USA, 1994.

18 Siemens, SHELXTL (v. 5.0), Siemens Industrial Automation, Analytical Instrumentation, USA, 1995.

19 A. E. Martell and R. J. Motekaitis, *Determination and Uses of Stability Constants*, VCH Publishers, New York, 2nd edn., 1992.

20 E. L. Mutterties and L. J. Guggenberger, *J. Am. Chem. Soc.*, 1974, **96**, 1748–1756.

21 J. Galy, J. I. Bonnet and S. Anderson, *Acta Chem. Scand. Ser. A*, 1979, **33**, 383–389.

22 E. Kimura, T. Shiota, T. Koike, M. Shiro and M. Kodama, *J. Am. Chem. Soc.*, 1990, **112**, 5805.

23 J. Suh, J. Son and M. P. Suh, *Inorg. Chem.*, 1998, **37**, 4872–4877.